

0012

DOT/FAA/CT-82/149

# Antimisting Fuel Breakup and Flammability

P. Parikh  
R. Fleeter  
V. Sarohia

Prepared for:  
Federal Aviation Administration, Department of Transportation  
through an agreement with  
National Aeronautics and Space Administration  
by  
Jet Propulsion Laboratory  
California Institute of Technology  
Pasadena, California 91109

December 1983

Final Report

This document is available to the U.S. public  
through the National Technical Information  
Service, Springfield, Virginia 22161.



U.S. Department of Transportation  
**Federal Aviation Administration**  
Technical Center  
Atlantic City Airport, N.J. 08405

1. Report No. DOT/FAA/CT-82/149	2. Government Accession No.	3. Recipient's Catalog No.	
4. Title and Subtitle Antimisting Fuel Breakup and Flammability		5. Report Date December 1983	
7. Author(s) P. Parikh, R. Fleeter, and V. Sarohia		6. Performing Organization Code	
9. Performing Organization Name and Address JET PROPULSION LABORATORY California Institute of Technology 4800 Oak Grove Drive Pasadena, California 91109		8. Performing Organization Report No.	
12. Sponsoring Agency Name and Address U.S. Department of Transportation Federal Aviation Administration Technical Center Atlantic City, NJ 08405		10. Work Unit No.	
15. Supplementary Notes		11. Contract or Grant No. DTFA03-80-A-00215	
16. Abstract The breakup behavior and flammability of antimisting turbine fuels subjected to aerodynamic shear are investigated in this report. Fuels tested were Jet A containing 0.3% FM-9 polymer (developed by ICI Americas) at various levels of degradation ranging from virgin AMK to neat Jet A. The misting behavior of the fuels was quantified by droplet size distribution measurements. A new technique based on high resolution laser photography and digital image processing of photographic records for rapid determination of droplet size distribution was developed for this purpose. The flammability of flowing droplet-air mixtures was quantified by direct measurements of temperature rise in a flame established in the wake of a continuous ignition source. The temperature rise measurements were correlated with droplet size measurements. The flame anchoring phenomenon associated with the breakup of a liquid fuel in the wake of a bluff body was shown to be important in the context of a survivable crash scenario. A new pass/fail criterion for flammability testing of antimisting fuels, based on this flame-anchoring phenomenon, was proposed. The role of various ignition sources and their intensity in ignition and post-ignition behavior of antimisting fuels was also investigated. Finally, the rate of flame spread on the surface of a pool of Jet A and AMK fuels was investigated for various depths of fuel layer at ambient temperature conditions.		13. Type of Report and Period Covered Final August 1981-1982	
17. Key Words (Selected by Author(s)) Aircraft Fires Antimisting Fuels Broadbase Fuels Combustion and Flammability		18. Distribution Statement This document is available to the U.S. public through the National Technical Information Service, Springfield, Virginia 22161	
19. Security Classif. (of this report) Unclassified	20. Security Classif. (of this page) Unclassified	21. No. of Pages	22. Price

## ACKNOWLEDGEMENTS

This report represents the results of research carried out at the Jet Propulsion Laboratory, California Institute of Technology under Contract NAS7-100, Task Order RD-152, Amendment 249, sponsored by the Department of Transportation, Federal Aviation Administration under Agreement No. DTFA03-80-A-00215. The authors extend their gratitude to Mr. Bruce Fenton, Project Manager at FAA Technical Center for his guidance and suggestions. The assistance of Messrs. W. Bixler, B. Green, and R. Smither in fabrication of apparatus and running of tests is gratefully acknowledged.

## TABLE OF CONTENTS

CHAPTER	PAGE
Executive Summary -----	ix
1. Introduction -----	1
2. Atomization and Flammability Measurements in the Mini Wing Shear Facility -----	4
2.1 Problem Statement and Research Goals -----	4
2.2 Experimental Procedure -----	4
2.3 Results and Discussion -----	6
2.4 Conclusions -----	14
3. Flame Stabilization and Flammability Criteria -----	15
3.1 Background and Literature Review -----	15
3.2 Description of the Apparatus -----	16
3.3 Results and Discussion -----	17
3.4 Role of Intensity and Type of Ignition Source -----	19
3.5 Conclusions -----	26
4. Flame Spread on the Surface of a Liquid Fuel Pool -----	27
4.1 Background -----	27
4.2 Apparatus and Procedure -----	27
4.3 Results and Discussion -----	33
4.4 Conclusions -----	33
References -----	36
Appendix A: Quantitative Measurement of Flammability in the Miniwing Shear Apparatus -----	37
Appendix B: Interpretation of Flammability Behavior as a Result of Classical Drop Combustion Behavior -----	38
Appendix C: Description of the Filter Ratio Test -----	40

LIST OF TABLES

	<u>Page</u>
Table 2-1    Mini Wing Shear Test Results: Jet A + 0.30 percent FM-9 -----	7
Table 2-2    Mini Wing Shear Test Results: Jet A + 0.25 percent FM-9 -----	8
Table 2-3    Mini Wing Shear Test Results: Jet A + 0.20 percent FM-9 -----	8

## EXECUTIVE SUMMARY

The breakup behavior and flammability of antimisting turbine fuels subjected to aerodynamic shear are investigated in this report. Fuels tested were Jet A containing 0.3 percent FM-9 polymer (developed by ICI Americas) at various levels of degradation ranging from virgin AMK to neat Jet A. The shearing air speeds employed ranged from 20 to 80 m/s (40 to 160 knots).

The misting behavior of the fuels was quantified by droplet size distribution measurements. A new technique based on high resolution laser photography and digital image processing of photographic records for rapid determination of droplet size distribution was developed for this purpose. The flammability of flowing droplet-air mixtures was quantified by direct measurements of temperature rise in a flame established in the wake of a continuous ignition source. The temperature rise measurements were correlated with droplet size measurements. The mist flammability, defined in terms of a reduced temperature, was found to be a function primarily of the mist SMD and was independent of the fuel dump rate.

The flame anchoring phenomenon associated with the breakup of a liquid fuel in the wake of a bluff body following ignition by a transient source was shown to be important in the context of a survivable crash scenario. A new pass/fail criterion for flammability testing of antimisting fuels, based on this flame-anchoring phenomenon, was proposed. Pass/fail boundary based on this criterion was found to be a strong function of both the airspeed and the degree of fuel degradation as measured by the filter ratio. Within the range of the fuel dump rates employed (10 to 40 gpm), it was not possible to have a self-supporting flame anchored in the wake of a bluff body (fail condition) for fuels having filter ratio larger than 8 and air speeds lower than 160 knots.

The role of various ignition sources and their intensity in ignition and post-ignition behavior of antimisting fuels was also investigated. It was found that the ignition source intensity plays a key role in determining whether or not ignition of a given droplet-air mixture will be achieved. The threshold ignition intensities to achieve ignition of various filter ratio fuels aerodynamically misted by a 100 knot wind were determined. Over a wide range of fuel dump rates and ignition source intensities in the present laboratory scale experiments, the proposed pass/fail criterion based on the flame anchoring phenomenon was found to be independent of the fuel dump rate and the ignition source intensity.

Finally, the rate of flame spread on the surface of a pool of Jet A and AMK fuels was investigated for various depths of fuel layer at ambient temperature condition. Within the uncertainty of the data, no significant difference between the flame spread rate over pools of Jet A and AMK fuels was observed. The flame spread rate generally increased from about 2 cm/sec to 3.5 cm/sec as the depth of the fuel layer was increased from 3 mm to 18 mm. The presence of a porous substrate (such as loosely packed soil) inhibits flame spread. Steady state flame spread over a fuel soaked bed of sand was 1/5 to 1/6 of the measured spread rate for a pure liquid layer.

## 1. INTRODUCTION

Fire related fatalities resulting from postcrash fires in otherwise survivable aircraft crashes are of a major concern to turbine powered commercial aircraft operations. Approximately 40 percent of the fatalities in such crashes are attributable to fire and fire-related effects (reference 1). Most postcrash fires are fuel-fed and the mechanism of their initiation, propagation and growth has been a subject of many investigations. Although a multiplicity of scenarios is possible, the most probable cause of a postcrash fuel fire has been identified as moderate to massive fuel spillage due to wing separation or fuel tank rupture during the dynamic phase of an impact survivable crash (references 1, 2). Currently employed commercial aircraft turbine fuels such as Jet A have typical wing tank temperatures well below the flash point and are difficult to ignite in bulk quantities. However, under dynamic crash conditions, when such fuels are released in moderate to large quantities from ruptured fuel tanks into a high speed airstream, they break up into fine droplets, thereby forming a highly flammable mist. This fuel mist is readily ignited by one or more of the numerous transient ignition sources such as friction sparks, electrical sparks, hot engine parts, etc. A rapid propagation of fire from transient ignition source to the point of fuel release occurs, accompanied by the development of a large fireball throughout the region of fuel mist. The fireball serves as a large ignition source that ignites pools of liquid fuel around the aircraft as it decelerates to a stop. The resulting pool fire is fed by additional fuel leaking from the damaged tanks and in some instances the rapid heating of undamaged fuel tanks results in explosions (references 1, 2).

A necessary precursor to the above chain of events in the development of a postcrash fire scenario is the misting tendency of the currently employed turbine fuels as they are released in a high speed airstream. If this misting can be suppressed sufficiently, the probability of ignition by transient ignition sources and subsequent fireball formation may be greatly reduced or eliminated, thereby preventing the entire large-scale, postcrash fire scenario. Polymer additives that impart such an antimisting property to currently employed turbine fuels have been developed over the last several years. An antimisting fuel offers its potential safety advantages during the short but critical dynamic (deceleration) phase of a survivable crash, thereby negating the entire postcrash, large-scale fire scenario.

With the development of polymer fuel additives that suppress the misting tendency, a need has arisen for the development of proper flammability test methods and meaningful pass/fail criteria to evaluate the fire suppression performance of these new antimisting fuels. Existing flammability criteria such as the flash point temperature are inadequate for this purpose. The use of flashpoint temperature to rate the flammability of various antimisting fuels containing the same base fuel (Jet A) but different additives (FM-9, AM-1, etc.) would lead to the erroneous conclusion that all antimisting fuels in this category are equally flammable, since the flash point temperature is not altered by the additives. The point is that any flammability test to evaluate the fire suppression performance of antimisting fuels should be realistic and should simulate as closely as possible the conditions that prevail during an actual crash.

Some insight into the events that lead to a large scale, postcrash fire scenario in a survivable crash may be gained from the NTSB accident reports

The JPL program on the investigation of the flammability of AMK fuel was designed to address all these important aspects of a survivable crash scenario. First, the misting behavior of fuels released in a high speed airstream was quantified by means of droplet size distribution and population measurements. A new technique based on high resolution laser photography and digital image processing of photographic records for rapid determination of droplet size distribution was developed for this purpose. Second, the flammability of a flowing droplet-air mixture was quantified by direct measurements of temperature rise in a flame established in the wake of a continuous ignition source. The temperature rise measurements were correlated with the droplet size measurements to demonstrate the role of misting in the flammability of droplet-air mixtures. Third, the flame anchoring phenomenon associated with the breakup of a liquid fuel in the wake of a bluff body was investigated and a new pass/fail criterion for flammability testing of antimisting fuels was proposed. The role of various ignition sources and their intensity in ignition and post-ignition behavior of antimisting fuels was also investigated.

Finally, the flame spreading rate on the surface of pools of Jet A and AMK fuels was investigated for various depths of the fuel layer at the ambient temperature condition.

The experimental configuration and results for each of the above four investigations are described separately in the following three chapters of this report.

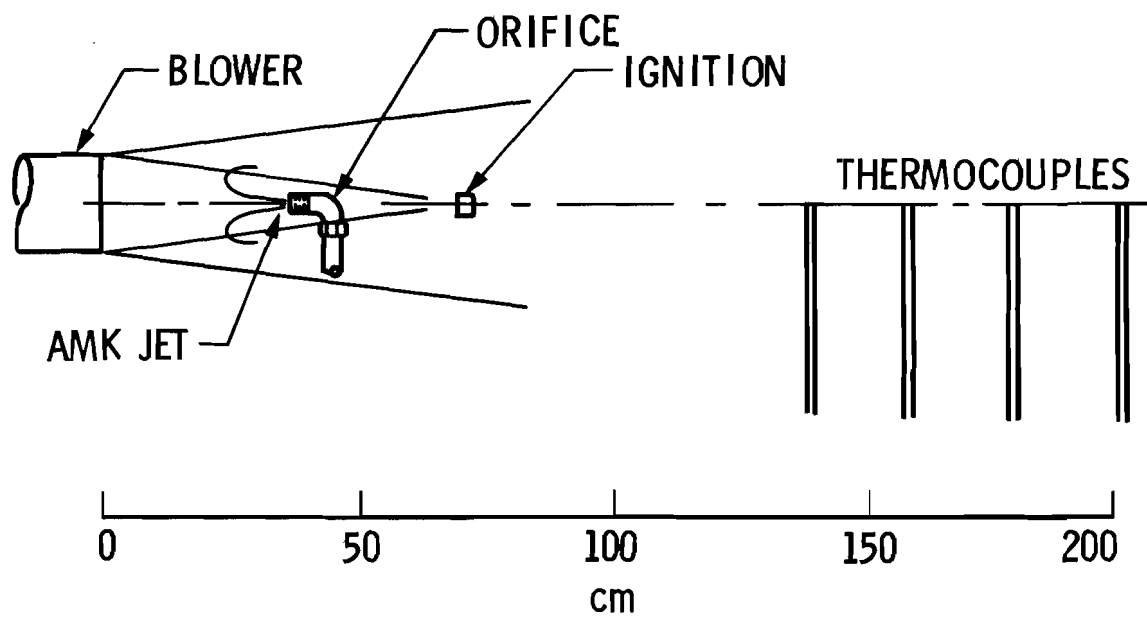


Figure 2-1. Mini Wing Shear Apparatus for Flammability Measurement

drops, 350 of the drops are under 50  $\mu\text{m}$  in diameter, even for 0.30 percent FM-9 AMK. The same spray is likely to contain only two or three drops over 1000  $\mu\text{m}$  diameter, and less than 20 drops over 500  $\mu\text{m}$  diameter.

In considering where the bulk of the fuel is, these few large drops are very significant. A hypothetical spray of 400 drops of 20  $\mu\text{m}$  diameter and 10 drops of 1000  $\mu\text{m}$  diameter has 99.97 percent of the fuel in the ten large drops. The SMD for this spray would be 985  $\mu\text{m}$ , reflecting the dominance of the 10 large drops out of the 410 drops counted. Despite their importance however, their relative scarcity means that not enough of them are counted to yield smooth population statistics. That is to say it is a matter of chance whether e.g., three rather than four large drops are observed in a sample of a negative. Observation of even 1 additional large drop may change the calculated SMD by several hundred microns (e.g., without the ten large drops the SMD of the hypothetical spray discussed above is reduced from 985 to 20  $\mu\text{m}$ ). This effect can only be eliminated by obtaining a large enough sample to observe a sufficient number of large drops to yield smooth statistics. This is not a practical solution as it requires counting about one hundred times as many drops as is done currently, a process requiring a man-week of work on each negative using the current system. Even such large-scale analytical effort might not yield smooth results as the breakup itself is inherently an unsteady process. An alternative is to artificially limit the maximum drop size to 1000  $\mu\text{m}$  diameter from 2000  $\mu\text{m}$ . This still permits sensitivity to most of the large drops carrying a significant portion of the fuel while eliminating those drops which by their random appearance distort statistical results.

Table 2-1. Mini Wing Shear Test Results: Jet A + 0.30 Percent FM-9

<u>Airspeed</u> m/s	<u>Fuel Flowrate</u> g/s	<u>SMD (2000 <math>\mu\text{m}</math> maximum diameter)</u> $\mu\text{m}$	<u>SMD (1000 <math>\mu\text{m}</math> maximum diameter)</u> $\mu\text{m}$	$\theta$
55	175	1243 $\pm$ 200	585 $\pm$ 50	0.005
55	520	822 $\pm$ 200	520 $\pm$ 50	0.0026
55	660	1036 $\pm$ 200	624 $\pm$ 50	0.001
81	175	1060 $\pm$ 300	564 $\pm$ 75	0.020
81	520	666 $\pm$ 300	494 $\pm$ 75	0.023
81	660	1245 $\pm$ 300	611 $\pm$ 75	0.020
99	175	1000 $\pm$ 400	656 $\pm$ 130	0.030
99	520	571 $\pm$ 400	571 $\pm$ 130	0.024
99	660	1348 $\pm$ 400	401 $\pm$ 130	0.018

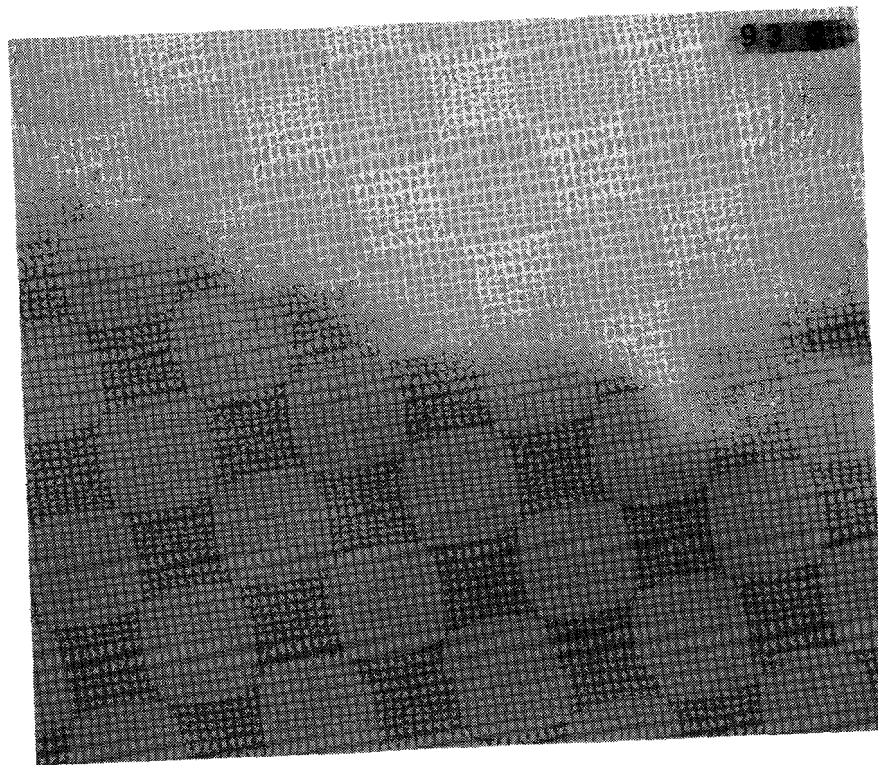


Figure 2-2. Mist Formed by Atomization of Jet A at  $97 \text{ m s}^{-1}$

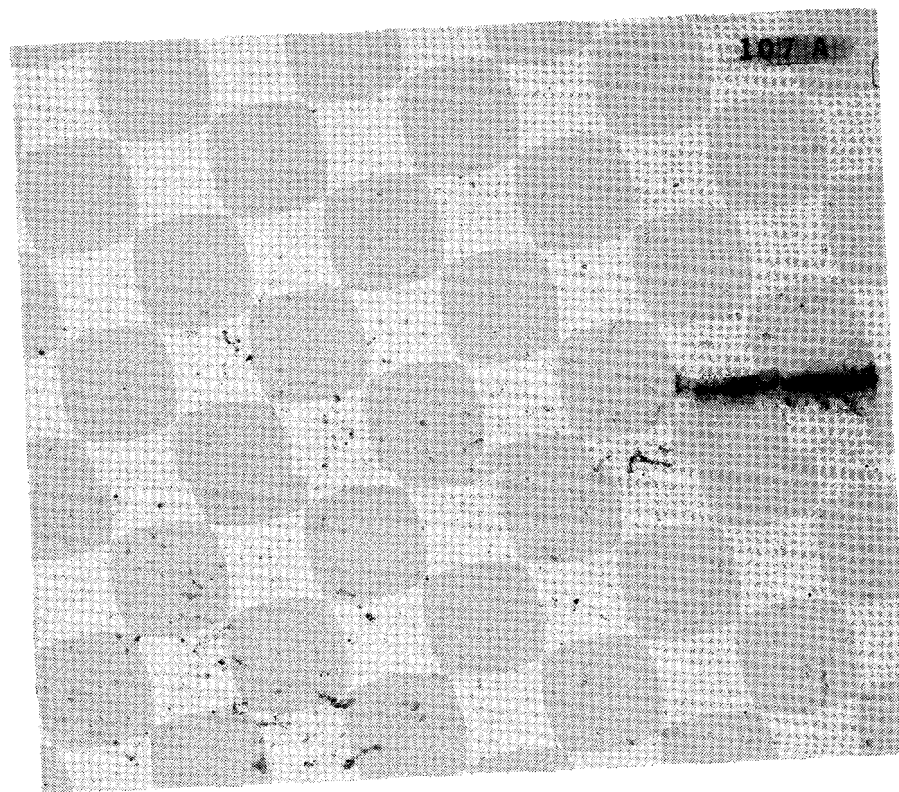


Figure 2-3. Mist Formed by Atomization of Jet A + 0.20% FM-9 at  $99 \text{ m s}^{-1}$

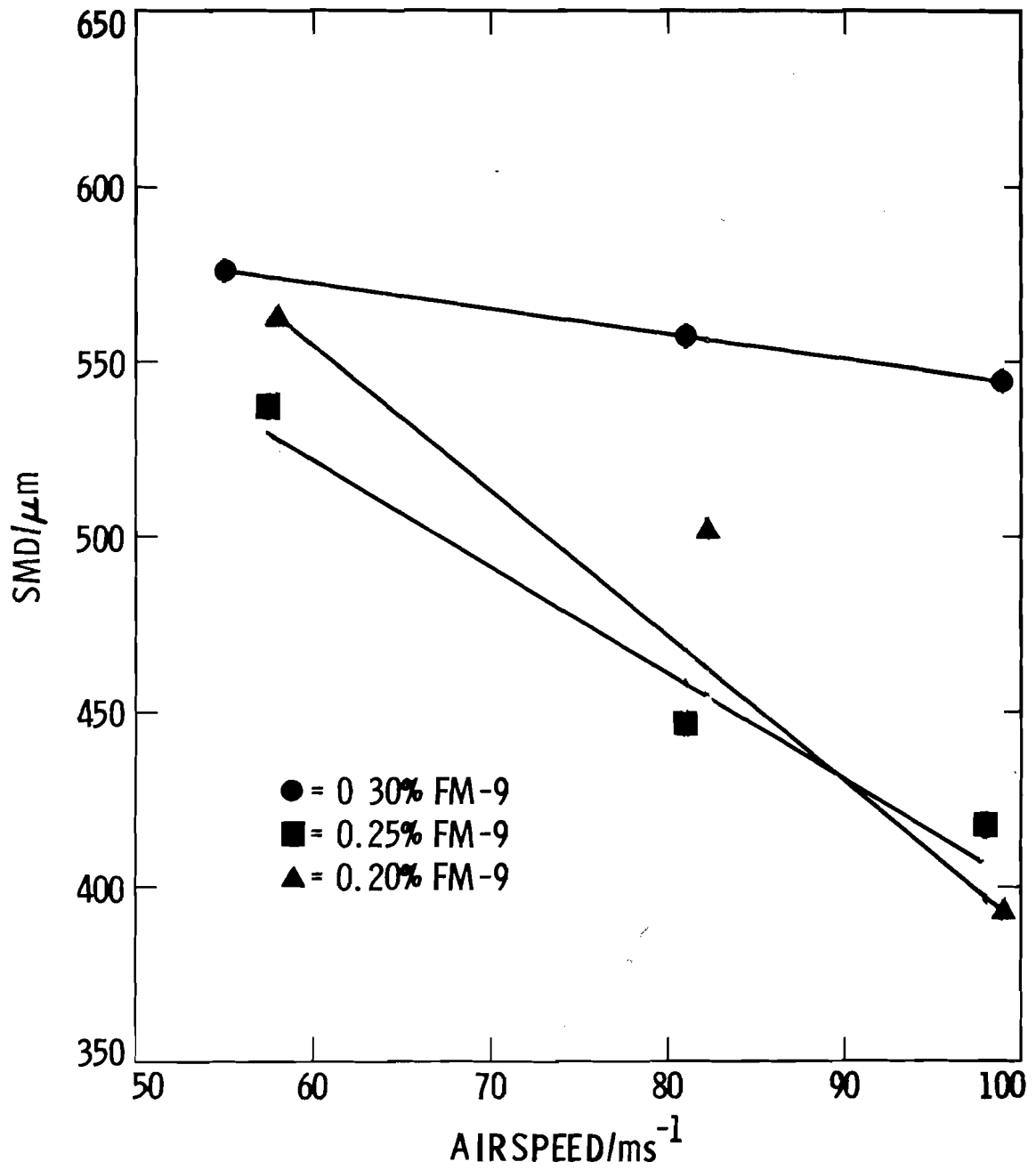


Figure 2-4. Fuel Atomization as a Function of Shearing Airspeed. SMD values computed with a maximum diameter of 1000 μm

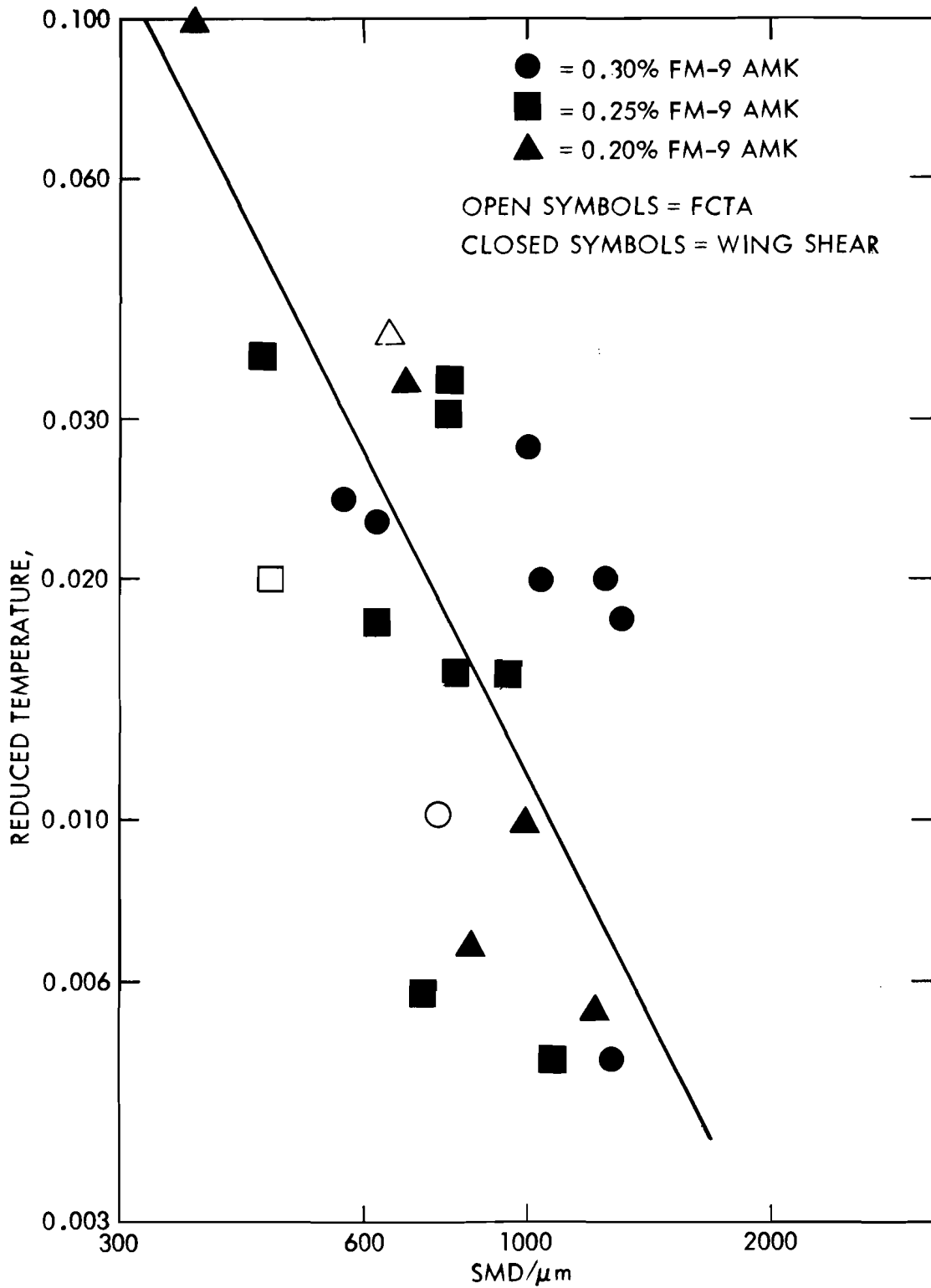


Figure 2-6. Comparison of Theory (straight line) and Experimental Flammability Results Linking Spray Flammability to Mist SMD. (The repeatability of the temperature measurements used in calculation of  $\theta$  is  $\pm 20\%$ . SMD Measurements carry an estimated uncertainty of  $\pm 100 \mu\text{m}$ -see text.)

### 3. FLAME STABILIZATION AND FLAMMABILITY CRITERIA

#### 3.1. Background and Literature Review

As mentioned in section 1 the existing test methods and criteria for evaluating the flammability of conventional turbine fuels are not suitable for testing antimisting fuels. New test methods and criteria within the context of a survivable crash scenario must be devised for such fuels. Several new test methods, all of which incorporate fuel droplet breakup by aerodynamic shear, have been developed over the years. Thus, all the new test methods incorporate the first important aspect of a survivable crash scenario discussed in section 1. However, the pass/fail criteria used in many of these tests are quite arbitrary. The tests thus serve as sorting tests, comparing the performance of one fuel with another on a certain scale peculiar to a given test. They do not provide a measure of the absolute fire resistance of the fuel as it relates to a survivable crash. One phase of AMK flammability work at JPL has been aimed at the development of an absolute pass/fail criterion, utilizing as a guideline the second important aspect of a survivable crash namely, the phenomenon of flame anchoring following ignition by a transient source as discussed in section 1. Before discussing the JPL work on the development of this pass/fail criterion of flammability, test methods and criteria employed by other investigators will first be reviewed.

Perhaps the most realistic flammability test is the RAE rocket sled test (reference 12). In this test, a wing shaped fuel tank is mounted on a sled and is accelerated to a desired speed along a track by means of rocket thrusters. The sled is then decelerated either by means of an arrester wire or by frictional means. In the "standard" test, decelerations as high as 10 to 25 g's are applied by means of the arrester wire, while "run on" tests employ frictional braking and produce decelerations of the order of 1 g. Fuel is allowed to spew out from a hole or slit in the leading edge of the wing tank during deceleration. In the "standard" test, the fuel is flung forward onto an array of ignition sources ahead of the sled, while in "run on" tests the sled passes in the vicinity of a series of ignition sources as it decelerates along the track. The test is considered fail or pass depending upon whether or not a large fuel fed fire results. The "run on" test is more representative of the Lakehurst simulated crash tests (reference 5) conducted by the FAA. The test requires a large apparatus and is relatively expensive to run.

Another intermediate scale flammability test is the wing spillage test described by San Miguel (reference 13) and Salmon (reference 14). Fuel is ejected under pressure from an orifice in the leading edge of a simulated wing against an airstream in a free jet wind tunnel and ignited by a propane torch located underneath the simulated wing. Many parameters such as airspeed, fuel flow rate, orifice diameter and fuel/air temperature could be varied. The criterion used for ascribing a pass or fail to a test was based on the rate of growth of fireballs as they convected downstream through the fuel mist. A fireball radius growth rate of 20 ft/sec or greater during a test was considered to be a fail condition while a value of 10 ft/sec or less was considered to be a pass. These limits were assigned after analyzing a great

duration of about 2 s while the sustained ignition source was an acetylene-air flame of varying intensity. The acetylene torch was ignited by means of the electrical spark during a test. If and when an ignition of the fuel droplet/air mixture was achieved, the acetylene torch was turned off. A key observation during a test was whether a stable, self-supporting flame fed by a freshly generated fuel droplets/air mixture could be established in the wing's wake following ignition either by the spark or by the acetylene torch.

### 3.3. Results and Discussion

The first series of tests was conducted with airspeed and orifice diameter as the parameters. Baseline flame anchoring data were obtained for Jet A fuel employing a short duration electrical spark as the ignition source. The data are presented in figure 3-1. Notice that at a fixed wing tank pressure (fuel jet velocity) whether or not a stable flame will result depends on the fuel jet diameter and the airspeed. The domains of pass and fail are separated in figure 3-1 by the dashed boundary.

Consider the behavior at a fixed orifice diameter as the airspeed is increased. At very low airspeeds, there is insufficient misting to achieve a spark induced ignition. As the airspeed is increased, the fuel jet begins to breakup into sufficiently fine droplets. Consequently, spark induced ignition of droplet-air mixture is achieved. More importantly, the resulting flame becomes anchored in the wing wake and in some cases envelopes the wing and is continuously fed by fresh droplet-air mixture generated by the disintegrating fuel jet. If the airspeed is increased above a certain value, spark ignition is once again not achieved as the number density of drops becomes too small. Ignition is not possible at any speed for orifice diameter of 1/4 in.

It should be mentioned at this point that similar upstream flame propagation and engulfment phenomenon was observed by Salmon (reference 14) in FAA wing spillage facility during tests with Jet A and underwing ignition. In some cases, flame propagated as far upstream as the fuel jet penetration distance. Motion pictures of this test sequence show remarkable similarity with the events of Lakehurst test No 1.

The flame anchoring tests were next conducted with AMK containing 0.3 percent FM-9 over the same range of airspeeds and jet diameters as employed in tests with Jet A. No ignition could be achieved over the entire test range when the ignition source employed was an electrical spark. An acetylene torch was next employed as the ignition source. The sequence of the test was as follows:

- 1) The blower was turned on and the airspeed was set at a desired value.
- 2) The fuel flow was turned on and fuel tank pressure adjusted to give the desired pressure in the wing tank.
- 3) Ignition was tried with spark source.
- 4) If unsuccessful, acetylene flow was turned on and torch ignition achieved with spark.

5) The acetylene-air flame then acted as a continuous ignition source.

Even with the maximum acetylene flow rate employed (0.157 l/s corresponding to heat release rate of 8.8 KW) ignition of virgin AMK containing 0.3 percent FM-9 was not achieved over the entire range of airspeeds and fuel jet diameters employed.

High speed motion pictures (400 frames/s) of the ignition and flame anchoring phenomena were taken during several of the Jet A tests described above. A close examination of these frames revealed that the boundary of the fuel jet after breakup reached the open air jet boundary and it appeared that flame stabilization in many cases may have occurred at the air jet boundary. Thus the shear layer surrounding the air jet acts as a flame stabilizer and influences the results of these tests. Such a shear layer does not exist in the vicinity of a wing moving through stationary air.

In order to alleviate the above ambiguity in the flame stabilization mechanism, it was then decided to use a bluff body flame holder. The streamlined wing was replaced by a 2 in. diameter cylinder placed with its axis normal to the free-stream direction as shown in figure 3-2. A recirculating flow behind the cylinder created an aerodynamic environment conducive to flame stabilization in its wake as seen in figure 3-3. With fuel ejected from an orifice at the leading edge of the cylinder, a stable, self-supporting flame could be established as seen in figure 3-4, provided the fuel droplet size was sufficiently small. A fixed orifice diameter of 1/2 in. was used in all the tests reported here. A 1.5 psi cylindrical tank pressure resulted in a fuel jet velocity of about 5 m/s or a fuel dump rate of 10 gpm for a 1/2 in. orifice. Three conditions were identified:

- 1) No ignition of fuel droplets was achieved.
- 2) Ignition of the fuel droplets was achieved, but the resulting flame was not self-supporting.
- 3) Ignition of the fuel droplets was achieved and the resulting flame was self-supporting.

The role of the type and intensity of the ignition source in the establishment of the above three conditions will next be discussed.

#### 3.4. Role of Intensity and Type of Ignition Source

The intensity and type of ignition source determines whether ignition of a given droplet-air mixture will occur. If the size and intensity of the ignition source are sufficiently large, ignition of any droplet-air mixture can be accomplished regardless of the droplet size. Thus the transition from condition 1 to condition 2 above is strongly dependent on the ignition source size and intensity. This was obvious from our tests, as the size and intensity of the ignition source was increased from an electrical spark to an acetylene flame of increasing heat release rate. In many instances, ignition was not achieved with a spark source and not achieved even with an acetylene

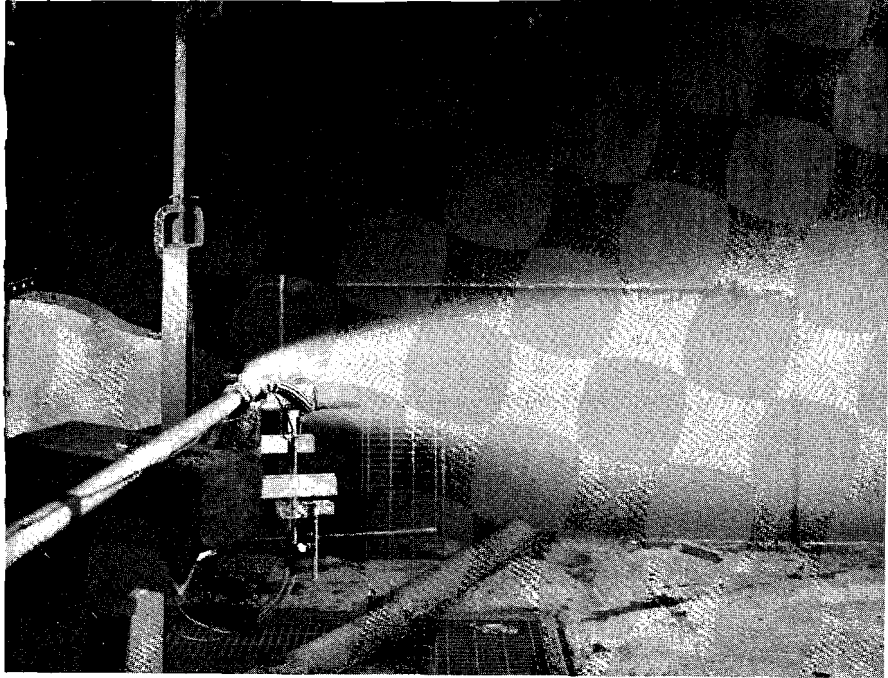


Figure 3-3. Fuel Jet Breakup in Flame Holding Experiments

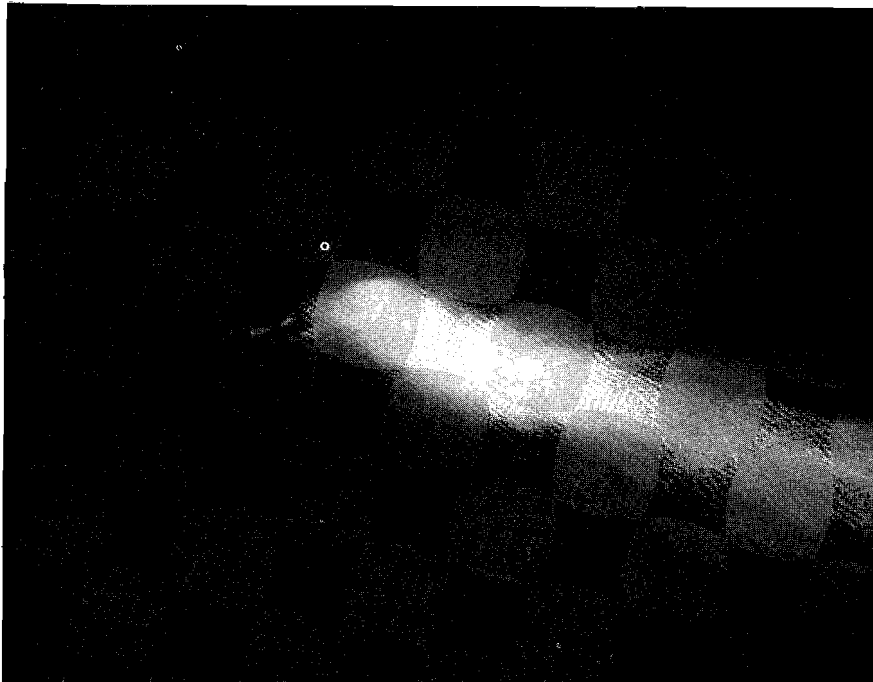
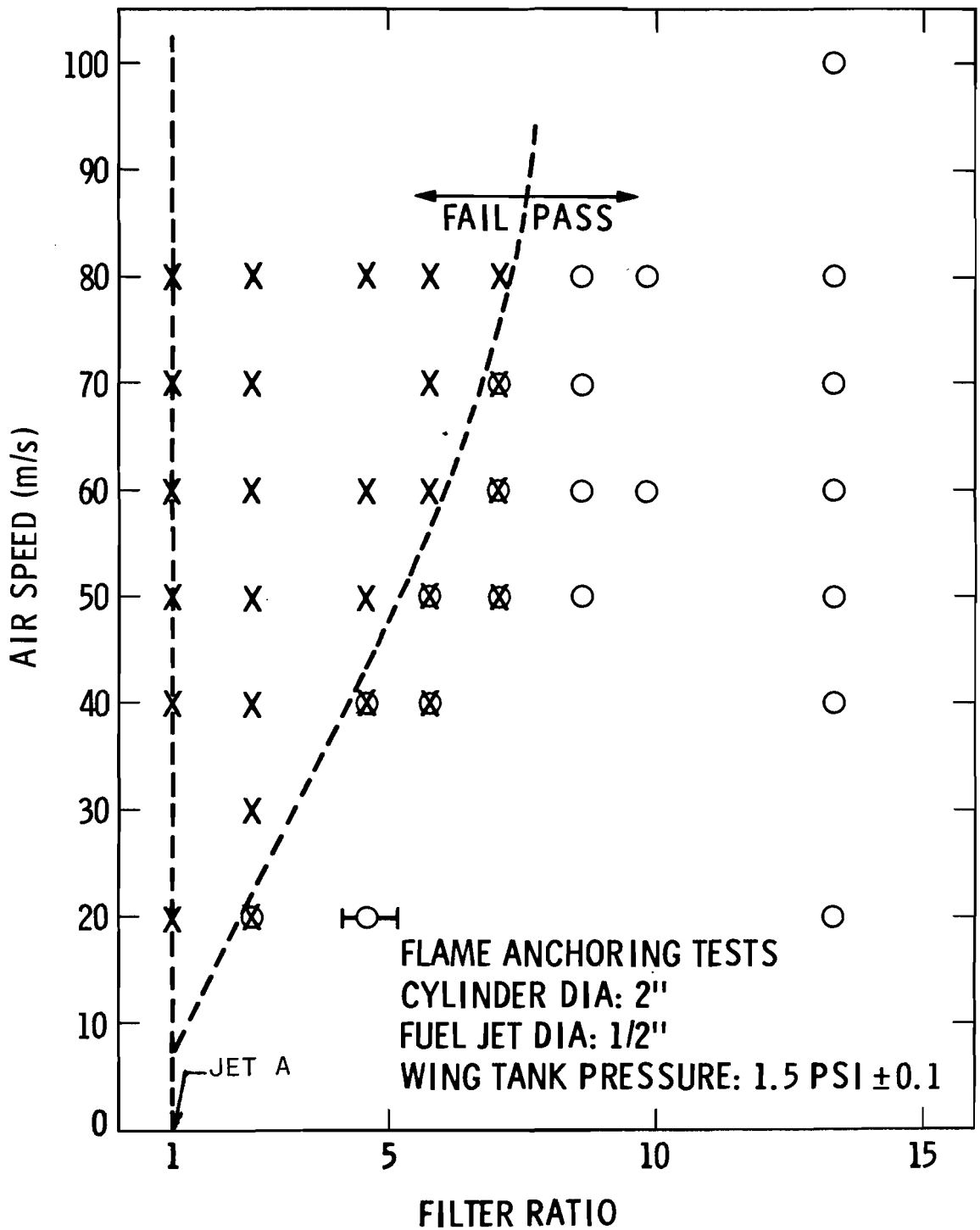
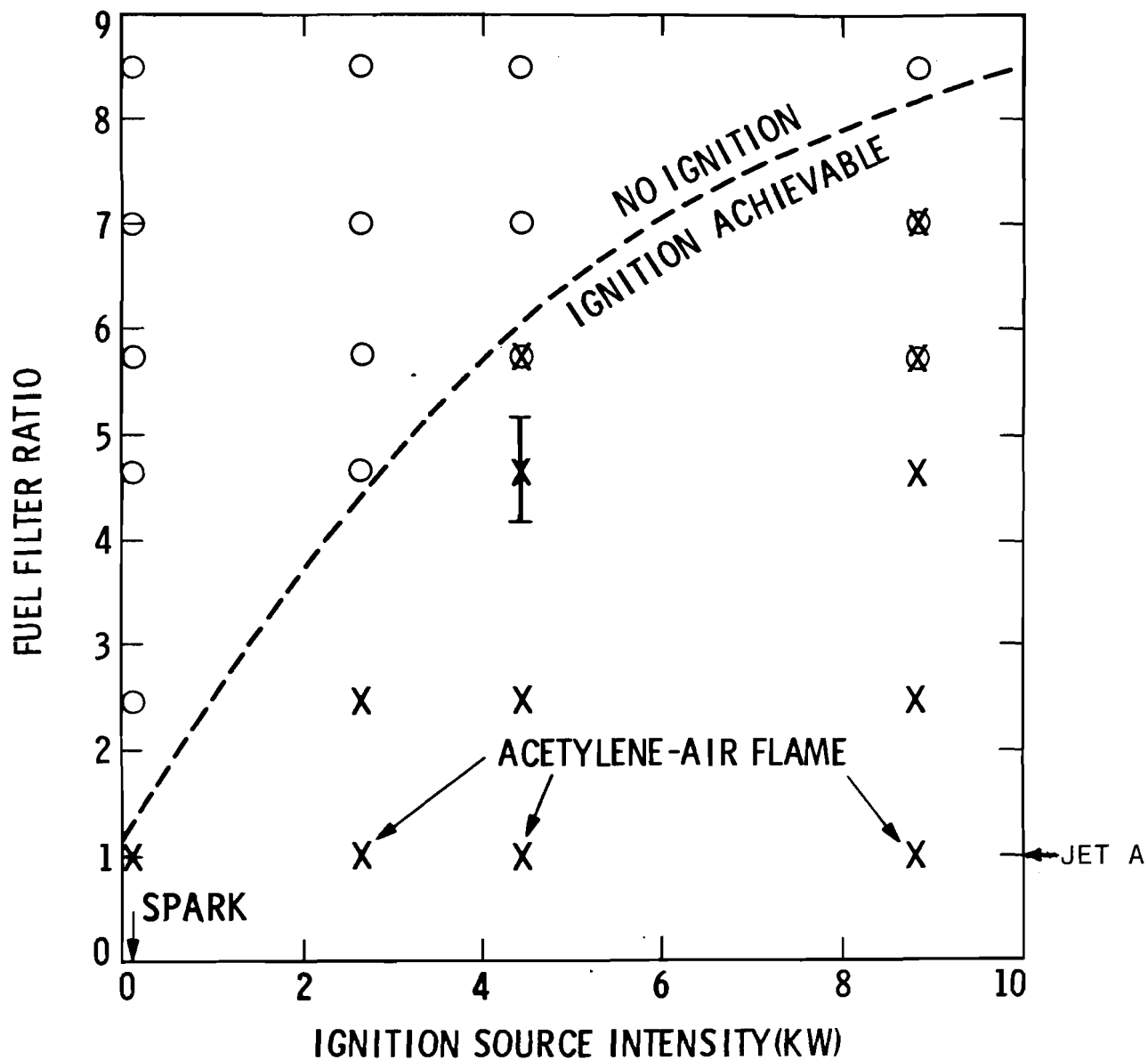


Figure 3-4. Flame Anchoring at  $U_{\infty} = 50$  m/s,  $FR = 4.65$



- LEGEND: ○ NO IGNITION ACHIEVED (PASS)  
 ⊗ IGNITION ACHIEVED BUT RESULTING FIRE NOT SELF-SUPPORTING (PASS)  
 X IGNITION ACHIEVED AND THE RESULTING FIRE SELF-SUPPORTING (FAIL)

Figure 3-5 Pass/Fail Boundary for Degraded AMK(0.3 percent FM-9) in Cylinder Flame Anchoring Experiments. Ignition Source: Acetylene-Air Flame, 8.8 KW



LEGEND: ○ NO IGNITION ACHIEVED (PASS)  
 ⊗ IGNITION ACHIEVED BUT RESULTING FIRE NOT SELF-SUPPORTING (PASS)  
 X IGNITION ACHIEVED AND THE RESULTING FIRE SELF-SUPPORTING (FAIL)

Figure 3-6 Threshold Ignition Source Intensity as a Function of Filter Ratio for Degraded AMK(0.3 percent FM-9)  
 $U_{\infty} = 50$  m/s

## 4. FLAME SPREAD ON THE SURFACE OF A LIQUID FUEL POOL

### 4.1. Background

As was discussed in chapter 1, the phenomenon of flame spread on the free surface of a liquid fuel pool is of considerable interest in the study of postcrash fire scenario. The rate of flame spread determines the rate of growth of fire intensity and hence the time available for safe evacuation of survivors.

Conventional aviation turbine fuels have flash point temperatures well above typical wing tank temperatures. Consequently, the flame spread rates over the surface of such fuels are much lower than those over the surface of low flash point fuels such as gasoline. For the latter type of fuels, a combustible mixture of fuel vapors and air already exists close to the free surface even at moderate to low ambient temperatures (0 to 30° C). Previous investigations of flame spread over the surface of high flash point fuels have shown that the principal mechanism of flame spread is convective heat transfer to the liquid fuel ahead of the flame front. Viscosity plays a key role in convective heat transfer through the liquid layer. Therefore, antimisting fuel additives, which essentially alter the rheological properties of the fuel may be expected to have influence on the flame spread rate over the liquid surface. The present investigation was undertaken to assess this influence. Flame spread rate measurements were carried out with the depth of the fuel layer as a parameter for both Jet A and AMK fuel containing 0.3% FM-9 additive. Initial fuel temperature is expected to have a strong effect on the flame spread rate. However, in the preliminary investigation conducted here, the effect of initial fuel temperature on the flame spread rate was not investigated systematically and all experiments were conducted at nearly the same initial temperature. The effect of the presence of a porous substrate on flame spread was also investigated.

### 4.2. Apparatus and Procedure

The apparatus consisted of a tray, 6 ft. long x 6 in. wide x 1 in. deep, fabricated from 1/8 in. stainless steel plate. The tray was welded onto an angle iron frame. Ten thermocouples, fabricated from 28 ga. chromel-alumel wire were placed six inches apart along the length of the tray. The thermocouples were supported by 1/8 in. stainless steel tubing which was inserted from the tray bottom through swagelok fittings. The swagelok fittings provided a leakproof seal around the 1/8 in. tubing, while enabling an adjustment of the junction height above the surface of the liquid fuel. During all the tests, the junction height was adjusted at 1/8 in. above the free surface for all thermocouples. A photograph of the instrumented tray used in the flame spread experiments is shown in figure 4-1.

The lead wires from the thermocouples were connected to a selector switch, which at a given position, connected the output of one of the thermocouples to a strip chart recorder. During operation, the selector switch was manually stepped progressively through the ten positions while monitoring the output at the strip chart recorder. When the temperature of a thermocouple being monitored rose above a certain level, the selector switch

was stepped to the next thermocouple position. The flame spread rate was slow enough so that this could be accomplished manually. A series of flame photographs is shown in figure 4-2 for different times during the flame spread process. Due to the fluctuations in the position of the flame front, combined with the finite response time of the thermocouples, the response at the strip chart recorder showed some fluctuations superimposed on an orderly temperature rise. During data reduction, a smooth curve was visually drawn through each temperature record to determine the time at which the response crossed a certain threshold temperature. The data were then plotted on an x-t diagram and the flame spread rate was determined therefrom by fitting a straight line through the data points. A sample strip chart record and the corresponding x-t diagram are shown in figure 4-3. Three test runs were conducted under identical conditions (fuel layer depth, fuel type) to check the repeatability of flame spread rate and to estimate uncertainty in the measurement.

At the beginning of each run, the tray was filled with fuel to a desired height. The tray was carefully leveled using spirit levels to ensure nearly uniform depth along the length of the tray. Due to warpage of the tray bottom during welding a variation of  $\pm 1/16$  in. in the measured depth of the liquid layer was introduced. To achieve a uniform depth of the fuel layer, previous experiments by McKinven et al. (reference 6) utilized a water substrate underneath the fuel layer. This technique could not be used in the present experiments due to the coagulation of the polymer additive upon contact with water. The thermocouple heights were then adjusted so that the junction protruded  $1/8$  in. above the liquid free surface. The initial air and fuel temperatures were recorded. An approximately 6 in. length of the tray from one end was then partitioned by means of a removable metal plate and the fuel in this compartment was ignited by means of an acetylene torch. Ignition was not achieved instantly, but required heating the fuel to a temperature above the flash point. Once the entire surface of the 6 in. compartment had been ignited, the metal plate partition was carefully removed (so that no waves were set up) and the flame was allowed to spread along the remaining free surface of the tray. The first thermocouple was encountered six inches down the tray axis from the initial flame front position after the partition was removed. When the flame had propagated the entire length of the tray, it was extinguished by means of a tray cover (figure 4-2) which cut off the air entrainment into the fire. The tray was then drained, washed and cooled with water and wiped clean to prepare for the next run. Five different fuel depths were used:  $1/8$  in.,  $1/4$  in.,  $3/8$  in.,  $1/2$  in. and  $3/4$  in. For fuel depths less than  $1/8$  in., it was not possible to maintain the flame--heat loss to the metal tray quenched the flame. A similar observation was made by McKinven et al. (reference 6).

A pair of tests were run to investigate flame spread on a porous substrate soaked with Jet A and AMK. During these tests, the tray was filled with a  $1/2$  in. layer of sand carefully packed and leveled with a flat surface. Fuel was poured over the sand until the substrate was saturated. Excess liquid on top of the sand layer was blotted off by means of absorbent tissue paper. Ignition was accomplished in the same manner as in the pure liquid layer experiments. It was found that the flame nearly failed to spread initially in the porous substrate experiments and continued burning locally for a considerable length of time. The localized fire was fed by fuel that seeped through the porous substrate. Eventually, however, due to conduction

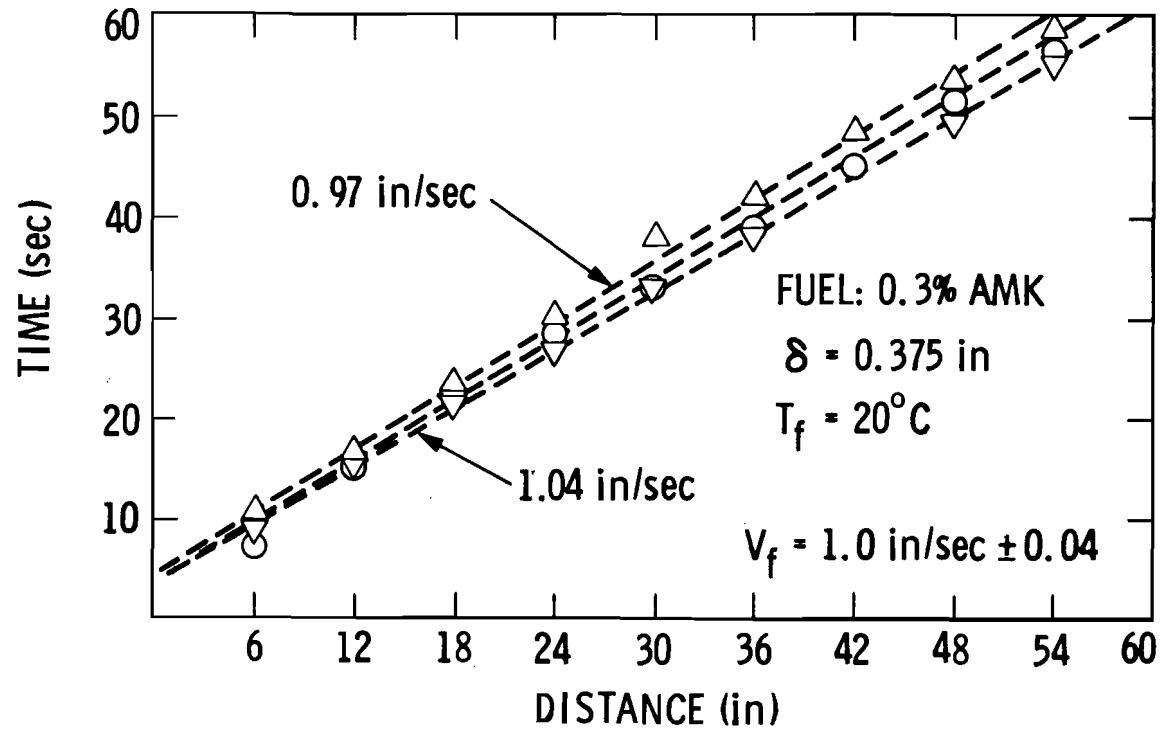
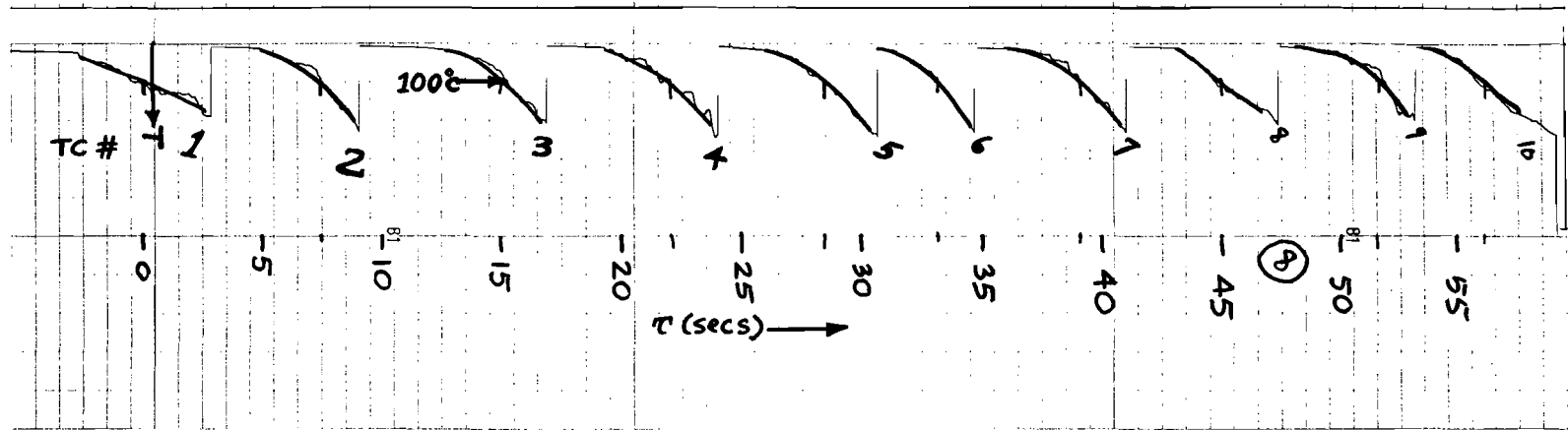


Figure 4-3. Sample Strip Chart Record and x-t Diagram for Flame Spread Tests

along the tray and radiation from the flame a slow spread began. The x-t diagrams for porous substrate experiments are shown in figure 4-4.

### 4.3 Results and Discussion

Flame spread rate data are plotted in figure 4-5 as a function of the liquid layer depth for Jet A and AMK containing 0.3 percent FM-9. In general the spread rate increases as the layer depth is increased. Within the uncertainty of the data, no significant differences between flame spread rate over Jet A and AMK fuel could be discerned.

The increase in the flame spread rate with fuel layer depth was most noticeable in the range  $3/8 \text{ in.} < \delta < 3/4 \text{ in.}$  For  $\delta < 3/8 \text{ in.}$ , the trend was somewhat erratic. This may be caused by the increasing role of conduction along the tray material as the fuel layer depth is decreased. At small depths, convection currents are suppressed but heating of the fuel ahead of the flame front is enhanced by conduction along the metal tray. At fuel layer depths less than  $1/8 \text{ in.}$ , the rate of heat loss to the tray is sufficient to quench the flame. Similar observation was reported by McKinven et al. (reference 6). The reason for increasing flame spread rate with increasing fuel layer depth was explained qualitatively by Makinven et. al (reference 6) as progressive reduction in viscous damping of surface currents by the tray bottom as the fuel layer depth is increased.

Also shown on Fig. 4-5 are the data of Eklund (reference 15) for Jet A and AMK containing 0.4% FM-4 additive. The flame spread rate measured by Eklund (reference 15) for Jet A is somewhat higher than that measured in the present investigation. This difference could be due to differences in the fuel composition (which affects flash point temperature), experimental apparatus and techniques used for spread rate measurement. The noticeable difference in the flame spread rate behavior between Jet A and AMK was not observed in the present experiments.

During experiments with a porous substrate, the initial spread rate of the flame was very slow following ignition by means of a propane torch. Initially the flame continued to burn almost locally with very little spread. However, as it began to grow in intensity, the radiation from the flame and conduction along the tray wall contributed to heating of the fuel ahead of the flame and spread rate increased. After some time the spread rate achieved a steady value (see Fig. 4-4) which was still  $1/5$  to  $1/6$  of the measured spread rate for a fuel layer in the absence of a porous substrate. The measured steady value of flame spread rate over a porous substrate was slightly lower for AMK (0.16 in/s) than for Jet A (0.21 in/s).

### 4.4 Conclusions

1. Within the uncertainty of the present data, no significant difference between the flame spread rate over pools of Jet A and AMK fuels was observed.

2. Over the range of fuel layer depths ( $\delta$ ) tested (1/8 to 3/4 inch), flame spread rate generally increased with increasing  $\delta$  from about 2 cm/sec to 3.5 cm/sec.

3. The presence of a porous substrate inhibits flame spread. Steady-state flame spread rate over a porous substrate soaked with fuel (Jet A or AMK) was 1/5 to 1/6 of the measured spread rate in the absence of the porous substrate.

## APPENDIX A.

### Quantitative Measurement of Flammability in the Miniwing Shear Apparatus

It is inherent to flammability testing that some intrinsic empiricism exists. As long as this is recognized and experimental repeatability is established, it is good experimental practice to use and rely on such heuristic data. An example of this approach within the AMK program is the use of the filter ratio (FR) as a measure of fuel degradation. The FR is defined as the time for a specific quantity of AMK contained in a vertically oriented, specifically designed container to pass through a particular filter under gravity, divided by the time for the same quantity of Jet A to do likewise. This test is highly precise (repeatability is high) and has found wide acceptance in the program despite the fact that it is completely heuristic and gives no information on the physical state of the polymeric solution it attempts to analyze.

In the case of flammability testing, the temperature along the jet centerline was measured with thermocouples of relatively slow response time ( $\sim 0.10$  s). The time-averaged maximum temperature along the jet axis is resolved and used as a measure of fuel flammability. No claim is made about the relationship of such a measure to specific physical data on fuel mist combustion except to rely on the observation that as a greater fraction of the fuel present in the mist is burned, the peak axial temperature increases. Similarly, we say that as the antimisting polymer is degraded, the FR decreases and hence conclude that FR is a measure of degradation. This peak temperature is corrected for the gross influence of changes in the fuel and air flows. As an example, identical experimental conditions (except for a doubling of the fuel injection rate) yield roughly a doubling of the observed temperature. This is felt simply to reflect the change in the amount of fuel present and not a fundamental change in fuel atomization or mist flammability. For these reasons a reduced temperature,  $\theta$ , was derived (see Appendix of Fleeter et al. 1981) as

$$\theta = \frac{\Delta T C_p \dot{M}_a}{\dot{M}_f q_f} = \frac{\dot{m}_f q_f}{\dot{M}_f q_f} = \frac{\dot{m}_f}{\dot{M}_f}$$

where  $\Delta T$  is the measured temperature rise,  $C_p$  is the (assumed constant) specific heat of air,  $\dot{M}_a$ , and  $\dot{M}_f$  are the air and fuel mass flow rates respectively,  $\dot{m}_f$  is the fuel consumption rate due to combustion, and  $q_f$  is the amount of heat released per unit mass of fuel consumed. Flammability results are all expressed in terms of this variable. While its value may be influenced by such factors as air entrainment and temperature distribution variation in the radial direction, the repeatability of the measure is well established (Fleeter et al. [reference 7]). Further, combustion of Jet A exhibiting a large fireball and leaving little residue except for considerable carbon soot typically yields values of  $\theta$  of about 0.6. Taken literally this implies that 60% of the fuel was burned to completion ( $H_2O$  and  $CO_2$  as the only products of combustion). In contrast, several tests with AMK yielded values of  $\theta$  around 0.01, indicating 1% of the fuel took part in combustion. This was accompanied with observation of large amounts of fuel residue in the form of liquid deposited on the facility walls and floor with a relatively small flame.

Thus from equations (7) and (8) we conclude

$$\epsilon = \frac{\dot{m}_f}{M_f} = \frac{\frac{\pi}{4} C_1 \rho_f \sum_i D_i}{\frac{\pi}{6} \rho_f \sum_i D_i^3} \quad (9)$$

i.e.

$$\theta \propto \frac{\sum D_i}{\sum D_i^3} \quad (10)$$

The quantity on the right side of equation 10 has dimensions of  $1/(\text{length})^2$ . If we use SMD of the spray as the characteristic length scale of the spray, this implies  $\epsilon \propto 1/(\text{SMD})^2$ . i.e.  $\log \theta \propto -2 \log (\text{SMD})$ . This relationship is shown as a straight line in Figure 2-6.

# DESCRIPTION OF FILTER SCREEN DEVICE

